Test of the Epstein−Plesset Model for Gas Microparticle Dissolution in Aqueous Media: Effect of Surface Tension and Gas Undersaturation in Solution

P. Brent Duncan and David Needham*

Department of Mechanical Engineering and Materials Science, Duke University, Durham, North Carolina 27708-0300

Received May 28, 2003. In Final Form: November 3, 2003

The gas from a free air bubble will readily dissolve in water, driven by two main factors: the concentration (undersaturation) of dissolved gas in the aqueous solution and the surface tension of the gas bubble−water interface via a Laplace overpressure in the bubble that this creates. This paper experimentally and theoretically investigates each of these effects individually. To study the effects of surface tension, single- and double-chain surfactants were utilized to control and define interfacial conditions of the microbubble in saturated solution. To study the effect of undersaturation, solid distearoylphosphocholine lipid was utilized to coat the gas microparticle with, essentially, a wax monolayer and to achieve zero tension in the surface. The experimental work was performed using a micromanipulation technique that allows one to create and micromanipulate single air microparticles (5−50 μm radius range) in infinite dilution and to accurately record the size of the particle as it loses volume due to the dissolution process. The micropipet technique has shown to be an improvement over other previous attempts to measure dissolution time with a 3.2% average experimental error in gas microparticle dissolution time. An ability to study a gas microparticle in infinite dilution in an isotropic diffusion field is in line with the theoretical assumptions and conditions of the Epstein−Plesset model. The Epstein−Plesset model on average underpredicted the experimentally determined dissolution time by 8.6%, where the effect of surface tension was considered with a range of surface tensions from 72 down to 25 mN/m. The Epstein−Plesset model on average overpredicted the dissolution time by 8.2%, where the effect of undersaturation was considered for a microparticle with zero tension in the surface (zero Laplace pressure) and a range of gas saturations from 70% to 100%. Compared to previous attempts in the literature, this paper more appropriately and accurately tests the Epstein−Plesset model for the dissolution of a single microbubble and an air-filled microparticle in aqueous solution.

Introduction

The study of how an air-filled microparticle behaves in aqueous suspension is important in many areas of current research and applications including the following: (1) ultrasound image contrast agents, where gas microbubbles and microparticles are strong scatterers of ultrasound waves used in diagnostic imaging of tissues and organs,[1−5] (2) decompression sickness, where gas nuclei and gas microbubbles may be the precursor to fully formed bubbles in the bloodstream,[6−9] (3) artificial oxygen carriers from lungs to tissue,[9−12] (4) drug/gene delivery vehicles,[13−18] and (5) chemical engineering and biotechnology mass transfer processes.[19−22] Underlying many of these phenomena is the dissolution of microbubbles in aqueous

* Corresponding author. E-mail: d.needham@duke.edu. Telephone: (919) 660-5355. Fax: (919) 660-5362.

(1) Blomley, M. J. K.; Cooke, J. C.; Unger, E. C.; Monaghan, M. J.; Cosgrove, D. O. Science, medicine, and the future − Microbubble contrast agents: a new era in ultrasound. *Br. Med. J.* **2001**, *322* (7296), 1222−1225.

(2) Goldberg, B. B.; Liu, J. B.; Forsberg, F. Ultrasound Contrast Agents − A Review. *Ultrasound Med. Biol.* **1994**, *20* (4), 319−333.

(3) Klibanov, A. L. Targeted delivery of gas-filled microspheres, contrast agents for ultrasound imaging. *Adv. Drug Delivery Rev.* **1999**, *37* (1−3), 139−157.

(4) Klibanov, A. L. Ultrasound contrast agents: Development of the field and current status. in *Contrast Agents II*; Springer-Verlag: Berlin, 2002; pp 73−106.

(5) Unger, E.; Shen, D. K.; Fritz, T.; Kulik, B.; Lund, P.; Wu, G. L.; Yellowhair, D.; Ramaswami, R.; Matsunaga, T. Gas-Filled Lipid Bilayers as Ultrasound Contrast Agents. *Invest. Radiol.* **1994**, *29*, S134−S136.

(6) Gerth, W. A.; Vann, R. D. Probabilistic gas and bubble dynamics models of decompression sickness occurrence in air and nitrogen−oxygen diving. *Undersea Hyperbaric Med.* **1997**, *24* (4), 275−292.

(7) Moon, R. E.; Vann, R. D.; Bennett, P. B. The Physiology of Decompression Illness. *Sci. Am.* **1995**, *273* (2), 70−77.

(8) Yount, D. E.; Strauss, R. H. Bubble formation in gelatin: A model for decompression sickness. *J. Appl. Phys.* **1976**, *47*, 5081−5089.

(9) VanLiew, H. D.; Raychaudhuri, S. Stabilized bubbles in the body: Pressure−radius relationships and the limits to stabilization. *J. Appl. Physiol.* **1997**, *82* (6), 2045−2053.

(10) Burkard, M. E.; Vanliew, H. D. Oxygen-Transport to Tissue by Persistent Bubbles − Theory and Simulations. *J. Appl. Physiol.* **1994**, *77* (6), 2874−2878.

(11) VanLiew, H. D.; Burkard, M. E. Bubbles in Circulating Blood − Stabilization and Simulations of Cyclic Changes of Size and Content. *J. Appl. Physiol.* **1995**, *79* (4), 1379−1385.

(12) VanLiew, H. D.; Burkard, M. E. Relationship of oxygen content to Po-2 for stabilized bubbles in the circulation: Theory. *J. Appl. Physiol.* **1996**, *81* (1), 500−508.

(13) Dayton, P.; Klibanov, A.; Brandenburger, G.; Ferrara, K. Acoustic radiation force in vivo: A mechanism to assist targeting of microbubbles. *Ultrasound Med. Biol.* **1999**, *25* (8), 1195−1201.

(14) Lawrie, A.; Brisken, A. F.; Francis, S. E.; Cumberland, D. C.; Crossman, D. C.; Newman, C. M. Microbubble-enhanced ultrasound for vascular gene delivery. *Gene Ther.* **2000**, *7* (23), 2023−2027.

(15) Lindner, J. R.; Kaul, S. Delivery of drugs with ultrasound. *Echocardiography−J. Cardiovasc. Ultrasound Allied Tech.* **2001**, *18* (4), 329−337.

(16) Porter, T. R.; Hiser, W. L.; Kricsfeld, D.; Deligonul, U.; Xie, F.; Iversen, P.; Radio, S. Inhibition of carotid artery neointimal formation with intravenous microbubbles. *Ultrasound Med. Biol.* **2001**, *27* (2), 259−265.

(17) Price, R. J.; Skyba, D. M.; Kaul, S.; Skalak, T. C. Delivery of colloidal, particles and red blood cells to tissue through microvessel ruptures created by targeted microbubble destruction with ultrasound. *Circulation* **1998**, *98* (13), 1264−1267.

(18) Schumann, P. A.; Christiansen, J. P.; Quigley, R. M.; McCreery, T. P.; Sweitzer, R. H.; Unger, E. C.; Lindner, J. R.; Matsunaga, T. O. Targeted-microbubble binding selectively to GPIIb IIIa receptors of platelet thrombi. *Invest. Radiol.* **2002**, *37* (11), 587−593.

(19) Bredwell, M. D.; Srivastava, P.; Worden, R. M. Reactor design issues for synthesis-gas fermentations. *Biotechnol. Prog.* **1999**, *15* (5), 834−844.

(20) Bredwell, M. D.; Worden, R. M. Mass-transfer properties of microbubbles. 1. Experimental studies. *Biotechnol. Prog.* **1998**, *14* (1), 31−38.

10.1021/la034930i CCC: $27.50
Published on Web 03/06/2004

media. A theory describing this gas bubble dissolution process was proposed by Epstein and Plesset in 1950.[23] While gas bubbles have been studied for many years, there is still a need to more accurately test Epstein and Plesset's (EP) original theory especially for gas microbubbles and gas microparticles. Thus, the experimental work reported here is motivated by this need to evaluate this theory and an opportunity to do so using a unique experimental micromanipulation technique. With this technique, we can study single microbubbles and gas microparticles of well-defined composition and in well-defined solution environments, conditions that match the EP-derived analytical solution for a single stationary free gas bubble dissolving (or growing) in a liquid−gas solution with and without surface tension.

The quasi-stationary model of Epstein and Plesset assumes that the velocity of the bubble interface (as it shrinks, for example, due to dissolution) can be neglected compared to the buildup of the boundary gas concentration layer, so that the convection term in the diffusion equation can be omitted. It will be shown for a gas microparticle that the steady-state assumption is valid given sufficient time for the gas concentration profile to become fully developed in the aqueous medium surrounding the microparticle (less than $^1/_{10}$ of a second). This derivation is presented next in the theory section. The change in size of the bubble is determined by the mass transfer and not governed by viscous or inertial forces.[24] Large bubbles (hundreds of micrometers range) change size relatively slowly in time due to gas saturation conditions or the Laplace pressure (in the kdyn/cm^2, milliatmosphere) range at these sizes. However, for gas microparticles in the tens of micrometers range, where the Laplace pressure is on the order of hundreds of kdyn/cm^2, the rate of volume change is easily measurable and recordable on a video microscope on laboratory time scales of tens of seconds. Producing and manipulating these gas microparticles using micropipet manipulation techniques is a main feature of the work we report in this paper.

We make the physical distinction between the two fundamentally different objects, a free gas microbubble and gas enclosed by a solid monomolecular shell, for experimentation and discussion. We therefore use "gas microparticle" as a general descriptor for free gas bubbles and gas encased in a shell (in this case made of solid-phase phospholipid, essentially a wax monolayer). Physically, the difference is that the free gas microbubble has a finite surface tension even when soluble surfactants are adsorbed at its surface, thereby lowering the surface tension. Therefore, a Laplace overpressure exists that drives gas out even when the surrounding aqueous gas concentration is saturated, while gas encased in a solid lipid shell has essentially zero tension in the surface, can persist in this equilibrium state, and so is only constrained by the gas concentration in solution. By creating gas microparticles where each of these two physical conditions of (1) a microbubble with defined surface tension in gas-saturated solution and (2) a shelled gas microparticle with zero tension in the surface in gas-undersaturated solution is met, we can experimentally test the variables of surface tension and gas concentration in solution, independently. Consequently, we are able to compare and contrast the predictions of the EP theory to well controlled and defined experimental conditions and measurable outcomes.

Since the theory appeared in 1950, there have been only a few attempts to measure the size of a single dissolving air bubble with time.[25−33] Basically, three methods have been used to observe the rate of dissolution of a stationary air bubble in water: the air bubble has been held in the medium under a horizontal glass plate, held by surface tension forces on a vertical plate, and held on a horizontal fiber. All these methods involve the influence of an impermeable boundary and therefore a nonisotropic diffusion and concentration field. Liebermann suspended a droplet of degassed water on the underside of a horizontal microscope slide, introduced a relatively large (initial radius, R_0 = 400−700 μm) air bubble by a pipet, and measured the diameter of the bubble at regular time intervals with a light microscope.[25] Similarly, Manley studied the dissolution of an air bubble (R_0 = 100−400 μm) in degassed water resting under the top plate of a pressure-controlled Perspex apparatus.[26] Houghton et al. viewed a pure gas bubble (R_0 = 100−250 μm) adhered (by surface tension) to the vertical side of a Perspex cell.[27] Wise and Houghton improved this latter method to facilitate bubble formation and allow the liquid temperature to range from 10 to 60 °C and viewed the bubble (R_0 = 100−200 μm) under a horizontal plate.[28] In another paper, Wise and Houghton again improved the precision of the last technique 5-fold by introducing only a single bubble (R_0 = 150−250 μm) in the cell.[29] Krieger et al.'s experimental method was to catch a bubble (R_0 = 100−300 μm) on a fine horizontal fiber and to photograph its projected image at given time intervals.[30] Ward et al.[31,32] have used a pressurizable apparatus to control the bubble size in order to define the initial state of the bubble and medium. While this experiment did improve upon past attempts, a quartz wire was still used to hold the position of the bubble and only data from an initial radius of 150 down to 60 μm were considered. Of all these experimental methods, none have taken surface tension into consideration (only dissolution via undersaturation), none of them have observed bubbles smaller than 100 μm initial radius, none of them controlled the surface composition and so had problems with contamination (often called an "organic skin"), and all of them had large error from the measurement and analysis method (±10% and higher).

(21) Kaster, J. A.; Michelsen, D. L.; Velander, W. H. Increased Oxygen-Transfer in a Yeast Fermentation Using a Microbubble Dispersion. *Appl. Biochem. Biotechnol.* **1990**, *24*−*5*, 469−484.

(22) Worden, R. M.; Bredwell, M. D. Mass-transfer properties of microbubbles. 2. Analysis using a dynamic model. *Biotechnol. Prog.* **1998**, *14* (1), 39−46.

(23) Epstein, P. S.; Plesset, M. S. On the stability of gas bubbles in liquid−gas solutions. *J. Chem. Phys.* **1950**, *18* (11), 1505−1509.

(24) Cable, M.; Frade, J. R. The influence of surface tension on the diffusion-controlled growth or dissolution of spherical gas bubbles. *Proc. R. Soc. London, Ser. A* **1988**, *420*, 247−265.

(25) Liebermann, L. Air bubbles in water. *J. Appl. Phys.* **1956**, *28* (2), 205−211.

(26) Manley, D. M. J. P. Change of size of air bubbles in water containing a small dissolved air content. *Br. J. Appl. Phys.* **1960**, *11*, 38−42.

(27) Houghton, G.; Ritchie, P. D.; Thomson, J. A. The rate of solution of small stationary bubbles and the diffusion coefficients of gases in liquids. *Chem. Eng. Sci.* **1961**, *17*, 221−227.

(28) Wise, D. L.; Houghton, G. The diffusion coefficients of 10 slightly soluble gases in water at 10−60 °C. *Chem. Eng. Sci.* **1966**, *21*, 999−1010.

(29) Wise, D. L.; Houghton, G. Diffusion coefficients of neon, krypton, xenon, carbon monoxide and nitric oxide in water at 10−60 °C. *Chem. Eng. Sci.* **1968**, *23*, 1211−1216.

(30) Krieger, I. M.; Mulholland, G. W.; Dickey, C. S. Diffusion coefficients for gases in liquids from the rates of solution of small gas bubbles. *J. Phys. Chem.* **1966**, *71* (4), 1123−1129.

(31) Ward, C. A.; Tucker, A. S.; So, C. W. A bubble evolution method for diffusion coefficient measurements utilizing the critical size concept. *J. Phys. Chem.* **1978**, *83* (4), 543−550.

(32) Ward, C. A.; Tucker, A. S. Thermodynamic theory of diffusion-controlled bubble growth or dissolution and experimental examination of the predictions. *J. Appl. Phys.* **1974**, *46* (1), 233−238.

(33) Borden, M. A.; Longo, M. L. Dissolution Behavior of Lipid Monolayer-Coated, Air-Filled Microbubbles: Effect of Lipid Hydrophobic Chain Length. *Langmuir* **2002**, *18*, 9225−9233.

Recently, Borden and Longo,[33] following the work of Kim,[34−36] attempted to evaluate the role of a lipid shell in the dissolution process and modeled a phosphatidylcholine (PC) lipid coated gas microparticle ($R_0 = 15-50\ \mu$m) in aqueous solution with the EP theory. They varied the saturated hydrophobic chain length (Di12PC−Di24PC) and found a constant resistance below Di18PC and then a monotonic increase in monolayer resistance to gas dissolution with increasing chain length after Di18PC. They attributed an observed relative reduction in the gas transport of their experiment, compared to the EP theory, to the monolayer resistance. However, their data do not account for the diffusion hindrance due to the microparticle dissolving against the solid boundary (glass microscope slide) at which the bubbles were observed. Such a boundary necessarily influences the gas concentration around the particle with a nonisotropic buildup of gas in solution on the side facing the boundary. Thus, as discussed by Borden and Longo, these data are not an absolute test but do reflect a relative trend in monolayer resistance due to solid-state lipid shells. Absolute data can only be measured and calculated by using a technique which does not involve a solid boundary or by using a model that accounts for the boundary.[37] To date, all techniques found in the literature involve a solid boundary to maintain the gas particle stationary and in view, and a few have tried to correct the theoretical model for the solid impermeable boundary. In 1957, Liebermann[25] approximated a correction to the theory using an analogy with the electrostatic theory of charged spheres to show the effect of the point contact (assuming a very small contact) of a bubble with an impermeable wall by introducing a geometry factor deduced from potential theory that reduced the diffusion coefficient by an empirical $\ln 2 = 0.693$. Practically, the contact of the bubble with the wall would be a finite area based on the buoyancy of the gas microparticle and adhesion and spreading due to surface tension of the bubble. Manley[26] observed this area and calculated an angle of contact to give a depressed volume factor. The total correction is the ratio of the mass transfer geometry factor to the volume factor. Wise and Houghton found the ratio for a water−Plexiglas system to be 0.686 theoretically[38] and 0.695 experimentally,[28] which are very close to the point contact approximation of 0.693. This equates to a $1/\ln 2 = 1.44$ increase in dissolution time and cannot be due to any other possible stabilization mechanisms including a monolayer resistance to gas transport. The impermeable boundary also impinges on the isotropic diffusion and concentration field. We have found similar results by observing a gas microparticle held stationary against a glass coverslip at the top of an aqueous solution. Our micropipet-based experimental design, presented here, has improved the precision and ability to establish and test gas microparticles under conditions specified in the EP model. An air microbubble can be created and held stationary in the center of the aqueous liquid microscope chamber via a micropipet, which more closely complies with the theoretical assumption that the bubble is in a symmetric diffusion field in an essentially, with respect to microparticle size, infinite medium, and moreover, its size can be created in the tens of micrometers range and its whole dissolution history can be followed down to almost complete disappearance.

In addition to the effects of air undersaturation, the effects of surface tension will also be investigated. By forming a monolayer of waxy lipids at the gas microparticle interface, we can reduce the tension in the surface to zero[35,39] and study the gas undersaturation effect in the absence of such tension. No data have been found in the literature for the complete dissolution time of a gas microparticle that has had its surface tension systematically changed by use of known concentrations of surfactants. Previous dissolution experiments have been limited by the fact that only very large bubbles have been observed (millimeter size scale) where surface tension has an insignificant effect due to the relatively small Laplace pressure of the large bubbles.[25,27] The controlled use of surfactants in our study also helped to control the surface contamination problem of earlier studies. Surface tension has been shown to be most important when the medium is near (or at) saturation and can be neglected at low air concentrations where driving forces for dissolution are large and dissolution times short.[24,40,41] However, it is obvious from a simple calculation of the Laplace overpressure that the surface tension becomes a significant factor when the bubble size is small (beyond the range of previous measurements). For a 15 μm radius bubble, the overpressure reaches almost 100 kdyn/cm^2 ($^1/_{10}$ of an atmosphere) and rapidly increases to almost 300 kdyn/cm^2 ($^1/_3$ of an atmosphere) when the radius is 5 μm. Therefore, this research investigates the dissolution of gas microparticles starting at an initial radius of 15 μm in order for the Epstein and Plesset approximation to more accurately apply.

While the Epstein−Plesset model essentially captures the gas dissolution process, others have since developed more detailed models that take into account the vapor pressure of the surrounding medium in the bubble, gas expansion, air as a multicomponent mixture, convection, and bulk and interfacial rheological properties.[40−42] However, these models all involve only numerical solution techniques and the additional complication may not be necessary or add much to the original theory in the case of a single gas microparticle. It will be shown that for our system and conditions, the Epstein and Plesset approximation fits well the experimentally determined dissolution times within the now reduced error of the experiment and known diffusion coefficient and solubility data from the literature.

Theory

Epstein and Plesset's model describes the dissolution behavior of a single spherical gas bubble in an infinite

(34) Kim, D. H.; Klibanov, A. L.; Needham, D. The influence of tiered layers of surface-grafted poly(ethylene glycol) on receptor−ligand-mediated adhesion between phospholipid monolayer-stabilized microbubbles and coated glass beads. *Langmuir* **2000**, *16* (6), 2808−2817.

(35) Kim, D. Mechanical Properties, Microstructure, and Specific Adhesion of Phospholipid Monolayer-Coated Microbubbles. Thesis, Department of Mechanical Engineering and Materials Science, Duke University, Durham, NC, 2000.

(36) Kim, D. H.; Klibanov, A. L.; Evans, E.; Needham, D. Viscoelastic properties of phospholipid monolayer shells on air microbubbles. *Biophys. J.* **1998**, *74* (2), A313.

(37) Simmons, R.; Duncan, P. B.; Needham, D.; Howle, L. Dissolution of a Bubble Against an Impermeable Wall: A Comparison of Theory with Experimental Data. In preparation.

(38) Wise, D. L.; Houghton, G. Effect of an impermeable wall on bubble collapse in diffusion coefficient measurements. *Chem. Eng. Sci.* **1968**, *23*, 1501−1503.

(39) Kim, D. H.; Costello, M. J.; Duncan, P. B.; Needham, D. Mechanical Properties and Microstructure of Polycrystalline Phospholipid Monolayer Shells − Novel Solid Microparticles. *Langmuir* **2003**, *19*, 8455−8466.

(40) Yung, C.-N.; DeWitt, K. J.; Brockwell, J. L.; McQuillen, J. B.; Chai, A.-T. A numerical study of parameters affecting gas bubble dissolution. *J. Colloid Interface Sci.* **1988**, *127* (2), 442−452.

(41) Weinberg, M. C. Surface tension effects in gas bubble dissolution and growth. *Chem. Eng. Sci.* **1980**, *36*, 137−141.

(42) Kloek, W.; Vliet, T.v.; Meinders, M. Effect of bulk and interfacial rheological properties on bubble dissolution. *J. Colloid Interface Sci.* **2001**, *237*, 158−166.

medium. Here, the equations are rederived, so they can be expressed in the dimensional forms of the laboratory frame (compared to the nondimensional forms of the original paper) for direct comparison with experiment. The gas concentration depends on both time and position in the surrounding liquid $c = c(r, t)$ and is described by Fick's second law of diffusion in spherical coordinates,

$$\frac{\partial c}{\partial t} = D\nabla^2 c = D\left(\frac{2}{r}\frac{\partial c}{\partial r} + \frac{\partial^2 c}{\partial r^2}\right) \tag{1}$$

where D is the diffusion coefficient of the gas in the medium. Assuming a large volume of surrounding solution relative to the volume of the bubble, the gas concentration at the bubble's surface ($r = R$) is in equilibrium with the gas in the bubble and is considered saturated, C_s, and the concentration at $r = \infty$ is the initial gas concentration in solution C_0. Solving eq 1 with these initial and boundary conditions yields the concentration gradient at the bubble boundary:

$$\left(\frac{\partial c}{\partial r}\right)_{r=R} = (C_0 - C_s)\left(\frac{1}{R} + \frac{1}{\sqrt{\pi D t}}\right) \tag{2}$$

The bubble mass rate decreases with the gas flux J out through the bubble's surface:

$$\frac{\mathrm{d}m}{\mathrm{d}t} = -4\pi R^2 J = 4\pi R^2 \rho \frac{\mathrm{d}R}{\mathrm{d}t} \tag{3}$$

where ρ is the density of the gas. The dissolution rate of the bubble, as measured by the experimental quantity of bubble radius, is then

$$\frac{\mathrm{d}R}{\mathrm{d}t} = -\frac{J}{\rho} \tag{4}$$

The flux is obtained from Fick's first law of diffusion:

$$J = -D\frac{\partial c}{\partial r} \tag{5}$$

Combining eqs 2, 4, and 5 yields the dissolution rate of a free gas microparticle in an unsaturated solution:

$$\frac{\mathrm{d}R}{\mathrm{d}t} = -\frac{D(C_s - C_0)}{\rho}\left[\frac{1}{R} + \frac{1}{\sqrt{\pi D t}}\right] \tag{6}$$

For convenience, this equation can be further modified. The ratio f is defined as the initial dissolved gas concentration to the concentration at saturation, $f = C_0/C_s$. According to Henry's law, the saturation concentration is proportional to pressure ($k_H = C_s/P_\infty M_w$) and therefore, by assuming ideal gas law ($\rho = M_w P_\infty/BT$), proportional to the density of the gas in the bubble ($C_s/\rho = k_H BT$), where P_∞ is the external pressure, M_w is the gas molecular weight, T is temperature, and B is the gas constant. Therefore, eq 6 becomes

$$\frac{\mathrm{d}R}{\mathrm{d}t} = -Dk_H BT(1 - f)\left[\frac{1}{R} + \frac{1}{\sqrt{\pi D t}}\right] \tag{7}$$

This equation consists of two parts as shown by the two terms in the brackets. The first term ($1/R$) is the steady-state part of the solution, and the second term is the transient part of the solution. The transient part is related to the time for the gas concentration profile in the aqueous medium surrounding the bubble to develop. According to random walk theory and Fick's first law of diffusion, the distance a particle travels is equal to the square root of $2Dt$. The time to reach a fully developed profile is about 0.06 s, assuming the concentration profile is fully developed when it reaches the initial radius of the bubble (15 μm). Since this time to develop is at least 2 orders of magnitude less than the total dissolution time, it is considered insignificant and is neglected in order to obtain the approximate rate of dissolution equation:

$$\frac{\mathrm{d}R}{\mathrm{d}t} = -Dk_H BT(1 - f)\left[\frac{1}{R}\right] \tag{8}$$

The radius of the steady-state equation for a small gas microparticle in gas-undersaturated solution with zero surface tension is then

$$R = \sqrt{{R_0}^2 - 2Dk_H BT(1 - f)t} \tag{9}$$

Rearranging eq 9 for the total time of dissolution t_d (the time it takes for the bubble to completely dissolve in solution) gives

$$t_d = \frac{{R_0}^2}{2Dk_H BT(1 - f)} \tag{10}$$

Gas concentration is not the only driving force for bubble dissolution. The curvature of the bubble's surface and the fact that a surface tension σ can exist at the interface create a pressure inside the bubble according to the Laplace equation:

$$\Delta P = \frac{2\sigma}{R} \tag{11}$$

The total pressure in the bubble therefore increases as R decreases. Assuming an ideal gas and including this Laplace overpressure due to surface tension yields

$$P_\infty + \frac{2\sigma}{R} = \frac{nBT}{V} \tag{12}$$

where n/V is the molar concentration. The gas density in the bubble can now be expressed as

$$\rho_b = \frac{M_w}{BT}P_\infty + \frac{2M_w\sigma}{BT}\frac{1}{R} = \rho + \frac{2M_w\sigma}{BT}\frac{1}{R} \tag{13}$$

The dissolution rate of the bubble with surface tension is found by combining eqs 7 and 13 and including the constants f and k_H:

$$\frac{\mathrm{d}R}{\mathrm{d}t} = -Dk_H BT\frac{1 - f + \dfrac{2M_w\sigma}{\rho BTR}}{1 + \dfrac{4M_w\sigma}{3\rho BTR}}\left[\frac{1}{R} + \frac{1}{\sqrt{\pi D t}}\right] \tag{14}$$

Equation 14 is equivalent to eq 7 when surface tension equals zero. This equation can also be simplified by assuming steady state as shown before by neglecting the second term in brackets and constant finite surface tension (not a function of radius).

$$\frac{\mathrm{d}R}{\mathrm{d}t} = -Dk_H BT\frac{1 - f + \dfrac{2M_w\sigma}{\rho BTR}}{1 + \dfrac{4M_w\sigma}{3\rho BTR}}\left[\frac{1}{R}\right] \tag{15}$$

Integration of this equation for an air-saturated solution ($f = 1$) yields

$$R^3 - {R_0}^3 + \frac{2M_w\sigma}{\rho BT}(R^2 - {R_0}^2) = \frac{6Dk_H M_w\sigma}{\rho}t \quad (16)$$

Rearranging eq 16 for the time of dissolution t_d at $R = 0$,

$$t_d = \frac{{R_0}^2}{3Dk_H}\left(\frac{R_0\rho}{2M_w\sigma} + \frac{1}{BT}\right) \quad (17)$$

The equations are retained in dimensional form to facilitate comparison with experimental data. For theoretical prediction, values for the diffusion constant of air in water and the Henry's law constant (saturation concentration limit) of air in water were found in the literature to be in the range of $1.75-2.00 \times 10^{-5}$ cm^2/s[43] and 0.744−0.826 mM/atm ($2.16-2.40 \times 10^{-5}$ g/cm^3),[44] respectively. The density of air is 0.0012 g/cm^3, and the molecular weight of air is 29 g/mol, with all values at the temperature of the experiment, 22 °C. The diffusion constant and solubility then have ranges of values that will be presented on the data plots and represent upper and lower bounds for these parameters.

Experimental Materials and Methods

Experimental Setup. The gas microparticles were manipulated and observed using a micropipet manipulation system. This system has been developed and used by us and others to measure the mechanical properties of cells and lipid bilayer vesicles,[45−52] equilibrium and dynamic surface and interfacial tension,[53,54] permeability of lipid membranes,[55−57] receptor−ligand-mediated adhesion,[34,58−60] and other mechanical and thermomechanical properties to characterize a bimolecular membrane[47,61−64] and other particles such as microhydrogels and gas microparticles[35,36,39,47] (see ref 65 for the most recent review). The micropipet station consists of an inverted optical microscope (Nikon Diaphot 200) outfitted with a microscope stage that accommodates two opposing pipet micromanipulators. A 40× objective (Nikon) was used along with a 15× eyepiece to further magnify the microscopic image on a video monitor (Sony). The micropipet pressure is controlled by a simple Becton Dickinson 5 mL syringe and is monitored by an in-line pressure transducer (Validyne, Northridge, CA). The microscope has been interfaced with a CCD camera (Optronics Engineering), a video cassette recorder (Panasonic SVHS), and a multiplexer (Vista Electronics, La Mesa, CA) to allow recording of pressure and temperature on a videotape and analyzing for data acquisition post experimentation using a video caliper system (Vista Electronics). Glass micropipets (0.75 mm × 0.4 mm × 6 in., A-M Systems, Inc., Everett, WA) were modified using a pipet puller (David Kopf Instruments, Tujunga, CA) and then cut on a microforge to an inner diameter of about 8 μm for the holding pipet and about 50 μm for the transfer pipet. Manipulation chambers were constructed from standard glass microscope slides (25 × 75 mm) and glass coverslips (no. 1, 22 × 30 mm) cut and joined together using optical cement and minimal silicone grease (vacuum grade) in the configurations shown in Figures 1−3. The temperature was controlled by the ambient air temperature and was nearly constant at 22 °C ± 1 °C in all experiments.

To evaluate the effectiveness of the Epstein−Plesset model for gas dissolution, taking into account, independently, both surface tension and undersaturation of gas in the aqueous phase, two types of experiments were performed. Experiment I was to test the effect of surface tension on the dissolution of a free gas microbubble in air-saturated solution. Experiment II was to test the effects of an air-undersaturated solution on dissolution of a lipid-coated gas microparticle with zero tension in the surface. Each experiment required a slightly different micropipet setup and monolayer composition at the gas microparticle interface.

Experiment I. For the air-saturated case, we used free gas microbubbles where their interfacial tension was controlled by the concentration and type of a particular surfactant in solution. Gas bubbles were formed and held by the same micropipet directly in the gas-saturated solution. A schematic (not to scale) of the chamber setup for air-saturated experiments is shown in Figure 1. The fluid dimension is 22 × 12 × 2 mm, the overall microchamber dimension is 22 × 75 mm, the pipet tip radius is about 4 μm, and the initial bubble radius is 15 μm.

Experiment II. For the air-undersaturated case where the gas microparticle was such that it had zero tension in the surface by virtue of a solid lipid monolayer, a double microchamber was constructed to hold two adjacent liquids to allow transfer of the microparticle from the gas-saturated solution to the gas-undersaturated solution (Figures 2 and 3). Each fluid dimension

(43) Himmelblau, D. M. Diffusion of dissolved gases in liquids. *Chem. Rev.* **1964**, *64*, 527−550.
(44) Reid, R.; Prausnitz, J.; Sherwood, T. *The Properties of Gases and Liquids*, 3rd ed.; McGraw-Hill: New York, 1977.
(45) Evans, E.; Skalak, R. *Mechanics and Thermodynamics of Biomembranes*; CRC Press: Boca Raton, FL, 1980.
(46) Kwok, R.; Evans, E. Thermoelasticity of large lecithin bilayer vesicles. *Biophys. J.* **1981**, *35*, 637−652.
(47) Evans, E.; Needham, D. Physical properties of surfactant of bilayer membranes: thermal transitions, elasticity, rigidity, cohesion, and colloidal interactions. *J. Phys. Chem.* **1987**, *91*, 4219−4228.
(48) Needham, D.; Nunn, R. S. Elastic deformation and failure of lipid bilayer membranes containing cholesterol. *Biophys. J.* **1990**, *58*, 997−1009.
(49) Evans, E.; Rawicz, W. Entropy-driven tension and bending elasticity in condensed-fluid membranes. *Phys. Rev. Lett.* **1990**, *64* (17), 2094−2097.
(50) Bo, L.; Waugh, R. E. Determination of bilayer membrane bending stiffness by tether formation from giant, thin-walled vesicles. *Biophys. J.* **1989**, *55*, 509−517.
(51) Waugh, R. E.; Song, J.; Svetina, S.; Zeks, B. Local and nonlocal curvature elasticity in bilayer membranes by tether formation from lecithin vesicles. *Biophys. J.* **1992**, *61*, 974−982.
(52) Zhelev, D. V.; Needham, D.; Hochmuth, R. M. A novel micropipet method for measuring the bending modulus of vesicle membranes. *Biophys. J.* **1994**, *67*, 720−727.
(53) Lee, S.; Kim, D.; Needham, D. Equilibrium and dynamic interfacial tension measurements at microscopic interfaces using a micropipet technique. 1. A new method for determination of interfacial tension. *Langmuir* **2001**, *17*, 5537−5543.
(54) Lee, S.; Kim, D.; Needham, D. Equilibrium and dynamic interfacial tension measurements at microscopic interfaces using a micropipet technique. 2. Dynamics of Phospholipid Monolayer Formation and Equilibrium Tensions at the water−air interface. *Langmuir* **2001**, *17*, 5544−5550.
(55) Bloom, M.; Evans, E.; Mouritsen, O. G. Physical properties of the fluid lipid bilayer component of cell membranes − a perspective. *Q. Rev. Biophys.* **1991**, *24* (3), 293−397.
(56) Zhelev, D. V.; Needham, D. Tension-stabilized pores in giant vesicles: determination of pore size and pore line tension. *Biochim. Biophys. Acta* **1993**, *1147* (1), 89−104.
(57) Olbrich, K. Water Permeability and Mechanical Properties of Unsaturated Lipid Membranes and Sarcolemma Vesicles. In *Mechanical Engineering and Materials Science*; Duke University: Durham, NC, 1997.
(58) Noppl-Simson, D. A.; Needham, D. Avidin−biotin interactions at vesicle surfaces: adsorption and binding, cross-bridge formation, and lateral interactions. *Biophys. J.* **1996**, *70*, 1391−1401.
(59) Evans, E. Detailed mechanics of membrane−membrane adhesion and separation. II. Discrete kinetically trapped molecular cross-bridges. *Biophys. J.* **1985**, *48*, 185−192.
(60) Evans, E. Detailed mechanics of membrane−membrane adhesion and separation. I. Continuum of molecular cross bridges. *Biophys. J.* **1985**, *48*, 175−183.
(61) Needham, D.; Evans, E. Structure and mechanical properties of giant lipid (DMPC) vesicle bilayers from 20 °C below to 10 °C above the liquid crystal−crystalline phase transition at 24 °C. *Biochemistry* **1988**, *27*, 8261−8269.
(62) Needham, D.; McIntosh, T. J.; Evans, E. Thermomechanical and transition properties of dimyristoylphosphatidylcholine cholesterol bilayers. *Biochemistry* **1988**, *27* (13), 4668−4673.
(63) Needham, D.; Zhelev, D. Use of micropipet manipulation techniques to measure the properties of giant lipid vesicles. In *Giant Vesicles*; Luisi, P., Walde, P., Eds.; Wiley: New York, 2000.
(64) Needham, D.; Zhelev, D. The mechanochemistry of lipid vesicles examined by micropipet manipulation techniques. In *Vesicles*; Rosoff, M., Ed.; Marcel Dekker: New York, 1996.
(65) Kim, D.; Needham, D. Lipid bilayers and monolayers: Characterization using micropipet manipulation techniques. In *Encyclopedia of Surface and Colloid Science*; Marcel Dekker: New York, 2002; pp 3057−3086.

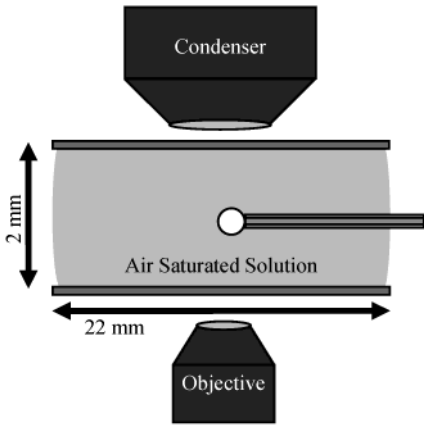

Figure 1. Side view (not to scale) of the microchamber setup for the air-saturated solution experiments (experiment I). The microbubble is formed and held with the pipet in the air-saturated solution. The initial bubble radius is 15 μm, the fluid dimension is 22 × 12 × 2 mm, and the pipet radius is about 4 μm.

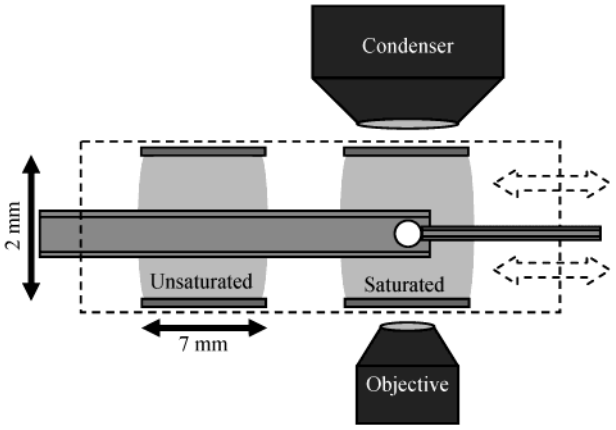

Figure 2. Side view (not to scale) of the microchamber setup for air-undersaturated solution experiments (experiment II). The gas microparticles were preformed in the air-saturated solution and then transferred to the unsaturated solution for dissolution measurement. Dashed arrows represent the lateral motion of the microscope stage, keeping the pipets and microparticle in constant focus. The initial bubble radius is 15 μm, the fluid dimensions are 7 × 12 × 2 mm, the transfer pipet radius is about 25 μm, and the holding pipet radius is about 4 μm.

is 12 × 7 × 2 mm, the overall chamber dimension is 22 × 75 mm, and the initial bubble radius is 15 μm. The phosphate-buffered saline (PBS) solution was initially degassed to about 0.7 saturation by placing 10 mL of PBS in a glass vial and placing it under a vacuum for 1 h in a glass desiccator. As soon as the vacuum was released, air necessarily began to diffuse back into the solution. To measure this rate of resaturation, the O_2 concentration was recorded in the microchamber as a function of time with a dissolved-oxygen meter (World Precision Instruments, Sarasota, FL) (Figure 4). The air concentration is 3 times the O_2 concentration. This is based on the assumption that O_2 and N_2 are the two main components and the knowledge that the partial pressure of N_2 is 4 times that of O_2 and the water solubility of O_2 is 2 times that of N_2. This setup allows for a known initial radius for the gas microparticle and initial conditions for the solution. For this experiment, gas microparticles had to be created with zero tension in their surface in order to eliminate the Laplace overpressure. No simple surfactant can achieve this state since exchangeable surfactants intrinsically produce lowered but nevertheless finite surface tensions (the lowest we attained was 30 mN/m with single-chain surfactants, and 25 mN/m was attained with liquid-phase phospholipids, see the next section). In previous experiments,[35,36,39] we have determined that a lipid

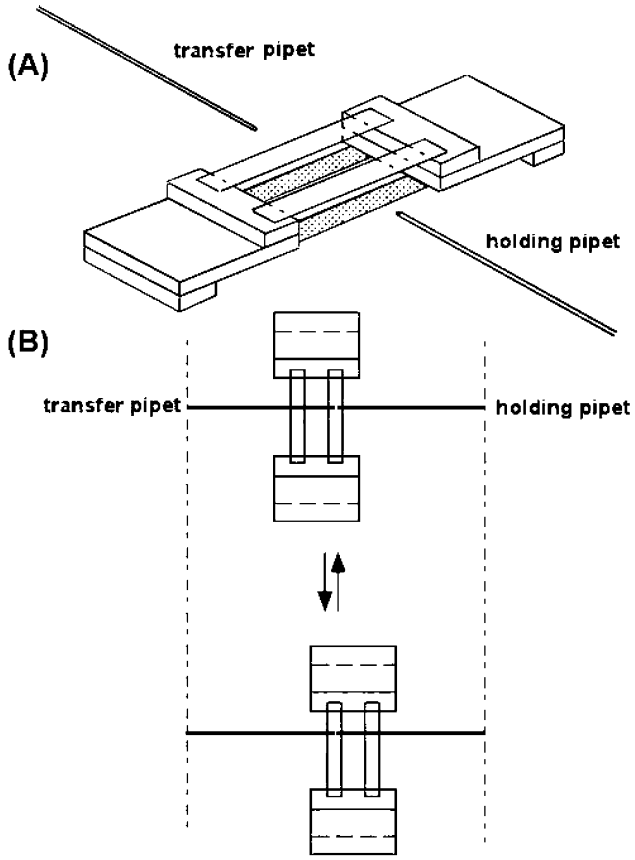

Figure 3. Transfer pipet experiment setup used for the undersaturated experiments (experiment II). Panel A shows the overall view of the setup, and panel B shows the top view of the chamber setup before and after moving the microscope stage (image from Dennis Kim, ref 35). Reprinted with permission from ref 35; copyright 2000 Duke University.

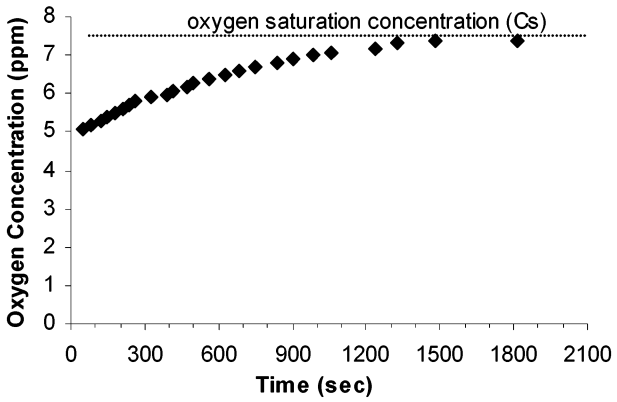

Figure 4. Gas resaturation concentration in the microchamber measured with a dissolved oxygen meter in the same position as the pipet after release of the vacuum at time 0.

shell formed at an otherwise free gas microbubble surface can, when converted into a waxy state by cooling the monolayer through its main acyl chain liquid−solid transition, essentially eliminate the tension in the surface and encapsulate the gas in a solid monomolecular thick wax shell. As described below, such wax (lipid) coated microparticles were preformed and added to the gas-saturated microchamber. To transfer the gas microparticle from its suspending gas-saturated solution into a solution of known gas undersaturation, two pipets are required, one for holding the air microparticle and one to act as a transfer pipet to transfer the microparticle across the air−water interface between the two microchambers without being exposed to ambient air,[57] as is explained in the experimentation setup section below.

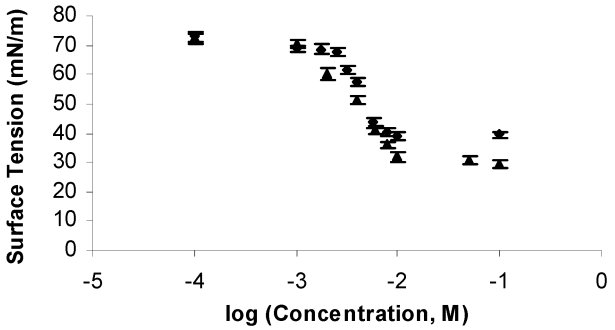

Figure 5. Surface tension of the air/water interface versus concentration of sodium dodecyl sulfate (diamonds) and dodecyl benzene sulfonic acid (triangles).

Materials. *Experiment I.* Common surfactants and lipids including sodium dodecyl sulfate (SDS), dodecyl benzene sulfonic acid (DDBSA), and the phospholipid stearoyloleoyl-phosphocholine (SOPC) were used to lower the surface tension of the gas bubble/aqueous solution interface. The surfactant samples were prepared by hydrating and dissolving a known dry surfactant mass with 10 mL of pure deionized water and diluting as necessary to produce the desired concentration. By controlling the concentration of the surfactant, the gas/water surface tension is set at prescribed values covering the range from pure water/air interface of 72 mN/m to that of the liquid-phase lipid monolayer at the air microbubble surface of 25 mN/m. The surface tensions of SDS and SOPC were found previously by using the micropipet manipulation technique.[53,54] The surface tension of DDBSA was used because of its ability to lower the surface tension to 30 mN/m, 10 mN/m lower than that of SDS, which allows for a wider range of experimentation. The surface tensions of SDS and DDBSA, measured using a micropipet technique, are shown in Figure 5 as a function of their concentrations in water.

Experiment II. A stable air microparticle was formed by creating a solid monolayer coating of a phospholipid that undergoes a phase transition from liquid to solid above the working temperature of room temperature. Distearoyl-phosphocholine (DSPC) was chosen because its transition temperature (55.1 °C[66]) allowed experimentation at room temperature while still possessing solid shell properties. The tension in the surface of the gas microparticle is zero, so the microparticle persists essentially indefinitely in gas-saturated solution, confirming the zero Laplace pressure. The DSPC monolayer, lipid-coated, air microparticles have been extensively studied and were produced as described previously.[35,39] Briefly, the main component of the shell was DSPC lipid (Avanti Polar Lipids, Alabaster, AL) along with a minor component for steric stabilization, poly(ethylene glycol)-40 stearate (PEG, Sigma, St. Louis, MO). The lipid/surfactant molar ratio was 10:1 (5 mM DSPC/0.5 mM PEG). The sample was probe sonicated (Mixonix model XL2020, Farmingdale, NY) to produce microparticles from entrained air. The sample was cooled from the elevated temperature caused by the sonication (70−80 °C) to room temperature (22 °C) at a rate of about 40 °C/min.

Experimentation Method. The free gas microbubbles and lipid-coated gas microparticles were held with a micropipet in the center of the aqueous solution as shown in Figures 1 and 2, respectively. This justified the assumption of a single, stationary gas microparticle in an infinite isotropic medium. The four videomicrographs in Figure 6 show the progression of the dissolution process.

Experiment I. For the gas-saturated solution case, the free gas microbubble was created with the holding pipet in water or surfactant solution by carefully blowing air from the pipet. The bubble was initially made to be slightly larger than the desired initial starting radius of 15 μm, usually about 17−20 μm. Once formed, the microbubble rapidly rose to the top of the chamber but was then easily captured by the micropipet at the top of the chamber and lowered to the center. The bubble was moved to a new position in the chamber to find fresh solution at gas-saturation concentration when its size reached 15 μm radius, and so the bubble was always in a known constant air concentration in water as a starting point for dissolution. Holding the microbubble in a stationary condition eliminated any washing effects due to convective transport.

(66) Marsh, D. *CRC Handbook of Lipid Bilayers*; CRC Press: Boca Raton, FL, 1990.

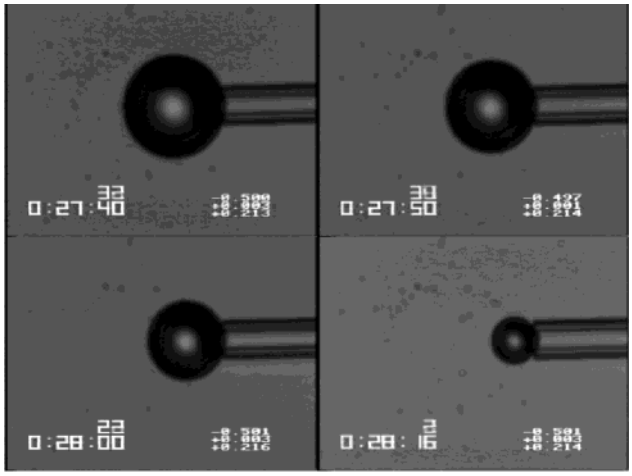

Figure 6. Videomicrographs of the dissolution of an air microbubble in 10 mM SDS solution held in the center of the chamber by a pipet with a suction pressure of 5 kdyn/cm^2 and solution temperature of 21.5 °C. The air bubble is shown at 15.0, 13.5, 11.0, and 3.5 μm in radius after 0 s (top left), 10 s (top right), 20 s (bottom left), and 36 s (bottom right), respectively.

To oppose the effects of buoyancy, the microbubble had to be held in the pipet with a small but significant suction pressure. Positioned at the end of the micropipet, the bubble simply dissolved in the saturated solution, losing volume at a rate readily measurable on the video recording. Then, once the bubble lost sufficient volume and reached the size of the pipet mouth, the bubble was sucked into the pipet. Thus the measurement could only be made down to about the size of the pipet (2.5−4 μm radius) and so required a small extrapolation to find the actual time of complete dissolution (radius → 0). Although only in the kdyn/cm^2 (milliatmosphere) range, the micropipet suction pressure was found to affect the time of dissolution; that is, the higher the suction pressure, the faster the dissolution of the gas from the bubble. This was corrected by performing an extrapolation of the dissolution time to zero suction pressure for three pressures of 20, 10, and 5 kdyn/cm^2. Therefore, two simple extrapolations are required to find the complete bubble's dissolution time when held with a pipet; that is, the first extrapolates the monotonic reduction in size from the pipet radius to zero radius, and the second takes these complete dissolution times as a function of pipet suction pressure and extrapolates a series of values from 20, 10, and 5 kdyn/cm^2 to zero pipet pressure.

Experiment II. For the undersaturated case and gas microparticles with zero tension in their surface, a few preformed lipid-coated gas microparticles were injected into the saturated solution where they remained stable for capture.[34−36,39] One was captured at the top of the chamber and lowered to the center. The transfer pipet was then translated to cover the bubble as shown in Figure 3. By moving the stage and keeping the gas microparticle in the transfer pipet, constantly centered and observable over the microscope objective, the external solution was changed from the saturated to the undersaturated solution, and the transfer pipet was moved away from the microparticle to expose it to the undersaturated solution. For comparison of experiments I and II, a lipid-coated gas microparticle (at zero tension in the surface) was also observed in saturated solution.

Results

Effect of Surface Tension (Experiment I). Figure 7 shows the data from a single experiment of air microbubble dissolution in 10 mM SDS solution. The three sets of points are the data at three different pipet suction pressures holding the air bubble (20, 10, and 5 kdyn/cm^2).

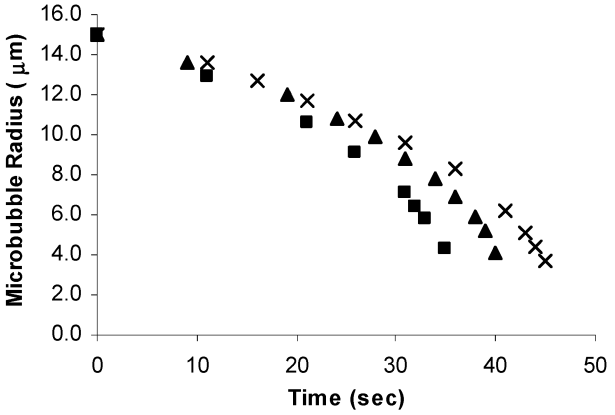

Figure 7. Effect of pipet suction pressure on surfactant microbubble dissolution. A 10 mM SDS example is shown of data from one experiment for a change of pipet suction pressure. The pipet inner radius is 4 μm. The pipet suction pressure in kdyn/cm^2 is 20 (■), 10 (▲), and 5 (×).

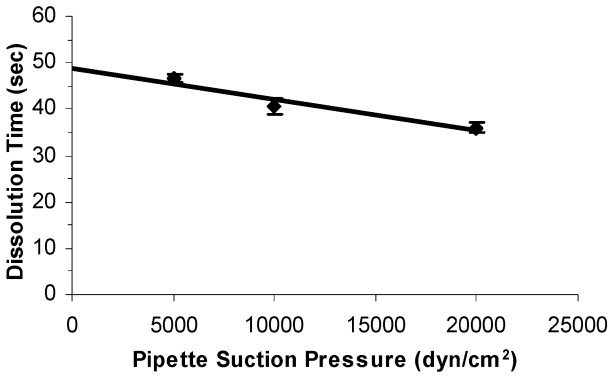

Figure 8. Zero pressure extrapolation of the three different micropipet suction pressures for the 10 mM SDS solution (from data in Figure 7).

Table 1. Concentrations and Type of Surfactants Used and Resulting Surface Tension

concentration	surface tension (mN/m)	concentration	surface tension (mN/m)
pure water	72	10 mM SDS	40
0.1 mM SDS	70	10 mM DDBSA	32
1.0 mM SDS	68	100 mM DDBSA	30
3.5 mM SDS	60	1 mM SOPC	25
4.5 mM SDS	50	5 mM DSPC (solid)	~0

This was repeated three times for each aqueous solution tested (see Table 1 for a list of solutions), and each solution was prepared three discrete times. This experimental setup allowed us to observe a gas microbubble in an essentially isotropic diffusion field and eliminated the anisotropic gas concentration gradient problems associated with an impermeable boundary, as exists if a microbubble is just allowed to rise and locate at the top of a glass microchamber. As explained in the previous section, each data set for a given pipet suction pressure was extrapolated to find the total time of dissolution at the particular pipet suction pressure. With a pipet radius of 4 μm, the microbubble could be followed almost to complete dissolution, so these three dissolution times are then linearly extrapolated to zero pressure (Figure 8). A total of 27 microbubbles were measured to obtain nine extrapolated dissolution times for each surface tension. To practically compare data from all the systems, the average of the nine extrapolated dissolution times is plotted against surface tension where all microbubbles had an initial starting radius at stationary conditions of 15 μm (Figure 9). The error bars represent the standard deviation of the nine extrapolated dissolution times. The shaded area represents the theoretical range resulting from the range of diffusion coefficient D and Henry's law constant k_H (solubility C_s) of air in water in the literature. The two outer lines of the shaded area were calculated from eq 17. The upper line represents the theory where the values are $D = 1.75 \times 10^{-5}$ cm^2/s and $k_H = 0.744$ mM/atm ($C_s = 2.16 \times 10^{-5}$ g/cm^3), and the lower line represents the theory where $D = 2.00 \times 10^{-5}$ cm^2/s and $k_H = 0.826$ mM/atm ($C_s = 2.4 \times 10^{-5}$ g/cm^3).

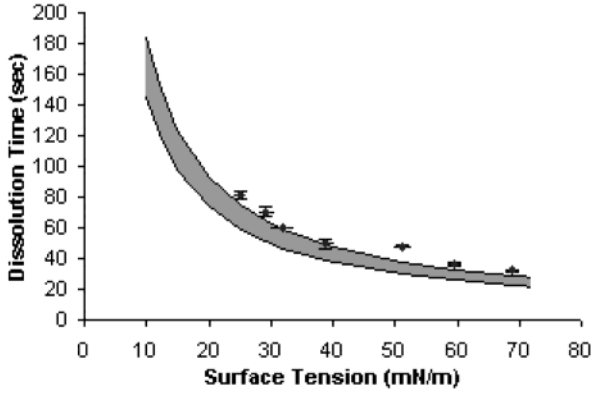

Figure 9. Experiment I and theory. Dissolution time for 15 μm radius air bubbles versus surface tension. The lines at the extremes of the shaded area represent the theory from eq 17 that result because of the range of D and k_H (C_s) of air in water in the literature.

Effect of Undersaturation (Experiment II). Utilizing gel-phase DSPC lipid as the monolayer shell surrounding the air microparticle permits the assumption to be satisfied of zero tension in the gas microparticle surface and with it, a condition of zero Laplace pressure. Gas dissolution is then only driven by the level of gas undersaturation in the surrounding solution. Starting with a maximally undersaturated solution, the undersaturated solution placed in the microchamber resaturates with air over time. Since the resaturation rate is relatively slow, this resaturation does not affect the gas microparticle dissolution once formed; it will only affect the initial conditions around the microparticle. As the air escaped from the gas microparticle, the solid-shelled monolayer was observed to be misshapen (crinkle) and reshape back to spherical caused by the buckling of the solid monolayer, possible folding and shedding of the lipid monolayer while still remaining contiguous with the interfacial material, and elastic recovery. Figure 10 shows the radius (measured at each spherical reshaping) versus time as the initial degree of saturation f. The degree of saturation f is the ratio of the initial air concentration in surrounding water to the saturated concentration of air in water. As the surrounding medium is more saturated with air (f is closer to 1), the particle dissolves at a slower rate. The saturated case ($f = 1$) is the same experiment as in the previous section (experiment I) with zero surface tension and has been tested to 6 h with no change in particle size and so essentially represents an infinite dissolution time and confirms the solid shell with zero tension in the surface and zero Laplace pressure. Figure 11 plots the average time of dissolution as a function of initial gas saturation. The average was calculated from seven dissolution times, and the error bars represent the standard deviation. The outer two lines of the shaded area represent the theory from eq 10 with upper and lower bounds of D and k_H (C_s).

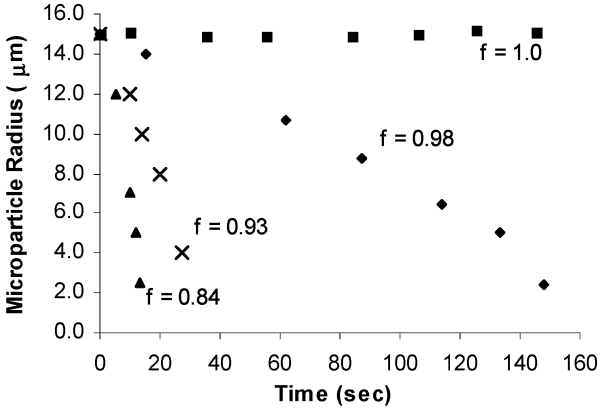

Figure 10. Effect of gas undersaturation for gas microparticles with zero tension in their surface (experiment II). Shown is the microparticle radius of the air-filled solid DSPC microparticle in an undersaturated solution with micropipet suction pressure of 20 kdyn/cm^2. The degree of saturation f is the ratio of the initial air concentration in surrounding water to the saturated concentration of air in water, and f is 0.84 (▲), 0.93 (×), 0.98 (♦), and 1.0 (■). The microparticle in the saturated solution ($f = 1$) is stable.

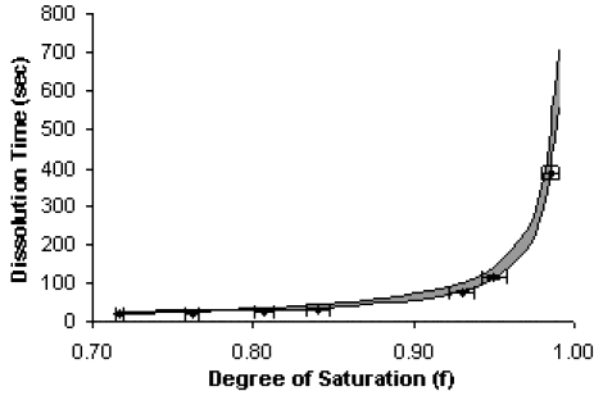

Figure 11. Experiment II and theory. Dissolution time of DSPC lipid coated 15 μm radius air bubbles versus the degree of air saturation of the medium f. The lines at the extremes of the shaded area represent the theory from eq 10 that result because of the range of D and k_H (C_s) of air in water in the literature.

Discussion

The micropipet technique was used to measure the dissolution of microbubbles (experiment I) and gas microparticles (experiment II) in aqueous media. The technique was shown to match the requirements and assumptions of the Epstein−Plesset theory. This micropipet technique has shown to be an improved method of measuring dissolution over previously reported attempts because microbubbles and microparticles can be created and held stationary in an essentially isotropic diffusion field, their dimensions measured accurately, and lifetime accurately found for complete dissolution. By using a controlled amount of suction pressure in a small pipet, microparticles can be easily manipulated in a solution. Microbubbles can be created with the pipet by applying a slight positive pressure and forcing air out into solution and the microbubble can then be held by a slight suction pressure, all with the same pipet. In addition, a preformed microparticle can be manipulated from the environment in which it was created (and in which it is stable) and transferred to a different environment for accurate measurement in a particular solution. The small pipet also allows the observation of almost the entire dissolution process. The entire microparticle dissolution experiment is recorded on a videotape for accurate measurement of the microparticle diameter, along with temperature and pressure indicators.

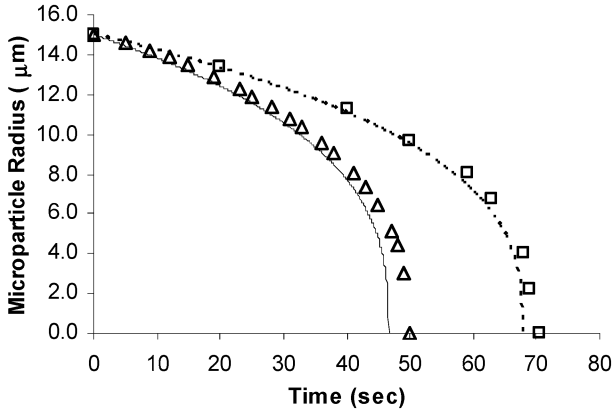

Figure 12. Dissolution of an air microbubble in saturated 10 mM SDS aqueous solution and influence of an impermeable boundary. The triangles represent the dissolution of a microbubble held with a micropipet in the center of the solution, while the squares are of a microbubble against an impermeable wall (top of the glass microchamber). The solid line represents the EP theoretical model, while the dashed line is the same EP theory modified with an empirically determined constant to correct for the diffusion against the impermeable wall.[23,25,26,28,38] The dissolution of an air microparticle against an impermeable wall lasts about 1.44 times longer, as empirically determined, than one held with a micropipet without this diffusion hindrance.

One of the most beneficial aspects of the micropipet technique is that it is free of any large solid boundary that greatly alters the isotropic diffusion process necessary for the theory. This technique eliminates the need for an impermeable boundary wall to hold the microparticle stationary in view and thus eliminates the hindrance of diffusion due to the impermeable wall. The only possible hindrance of diffusion is the pipet itself. It will have some hindrance of diffusion, albeit much smaller, due to the small surface area covered by the glass of the pipet tip. Dissolution data for a microparticle, which was not manipulated with a pipet but rather was allowed to float to the glass surface at the top of the experimental setup, have also been completed. Both experiments I and II were repeated with the microparticle allowed to rest against the glass microscope coverslip at the top of the chamber. All of these data will be presented in a future publication along with a new computational theory describing the effect of the impermeable wall on microbubble dissolution.[37] The computation model will fully describe the complex situation of gas diffusion from a microbubble against an impermeable wall. For the purpose of this discussion, a comparison plot of one microbubble held with the pipet and one resting against a horizontal glass microscope coverslip is shown in Figure 12. The EP theory is also plotted with average D and k_H found in the literature to show the comparison with a microbubble held with the pipet. The same EP model is multiplied by the previously found empirical constant of ln 2 (≈0.69) for comparison of the microbubble against the impermeable wall.[25,26,28,38] The modified EP theory is equivalent to a reduction of the diffusion constant by 0.69. The experimental data clearly demonstrate the relatively large change in dissolution time due to the impermeable wall. The microparticle against the impermeable wall does indeed increase the dissolution time by about 1.44, as approximated from the empirical correction calculated in the 1950s and 1960s. The empirical correction for the impermeable boundary wall, as shown previously, will increase the dissolution

time by 44%, compared to a free microparticle. This confirms the importance of using experimental conditions consistent with the theory in order to make absolute conclusions based on a theory. Thus, even with the small influence of the pipet and the necessity to use a pipet suction pressure, the micropipet technique mimics, as closely as possible, the EP theory for a free gas microbubble or gas microparticle in an isotropic stationary diffusion and concentration field.

Effect of Surface Tension (Experiment I). The aim of experiment I was to study the effect of surface tension on microbubble dissolution and compare it to the EP theory. The level of saturation of the solution surrounding the microbubble was constant at equilibrium saturation in all experiments, so the only mode of dissolution was due to surface tension alone. Single- and double-chain surfactants were used to produce an interface with a well-defined specific surface tension. The surface tension was adjusted by first choosing an appropriate surfactant and then by changing the concentration of surfactant in the aqueous solution prior to creating the microbubble. The surfactant also controlled any possible contamination at the interface, which if not controlled would form a "dirty skin" and necessarily change the dissolution rate, as found previously by others. The microbubble was produced in a well-defined environment and then held with a micropipet during dissolution. By controlling the interfacial properties, allowing essentially isotropic diffusion, and accurately measuring the microbubble size, the average experimental error was calculated to be 3.2% (percent standard deviation). This error is an improvement of the 10% or more found previously by others.

Without any fitting, the theory slightly underpredicts the dissolution time of experiment I by an average of 8.6% as shown in Figure 9. This is equivalent to only an average of a 4.4 s shift of the theory from the experimentally determined dissolution time for a 15 μm gas microbubble. The slight deviation of the theory from the experiment could be contributed by a few factors not incorporated in the original approximate theory. The factors include a possible monolayer hindrance to gas transport out of the gas microparticle, viscosity and elastic interfacial effects, solvent vapor pressure, and bulk viscosity effects. Previously these factors have been theoretically investigated by others using various numerical methods and it was shown that over most of the time domain of bubble dissolution the rather simple quasi-stationary model (in which the listed factors above are ignored but where surface tension effects can be easily accounted for) provides results which are very similar to a solution of the complex "complete" set of mass transfer equations.

Single-chain surfactants have been shown to have no effect on the rate of absorption of gases in water and are not considered a diffusion barrier.[25,27] Therefore, the surfactants used in experiment I (SDS and DDBSA) are not expected to cause a barrier to dissolution but would slow dissolution (compared to without surfactant) due to the lower surface tension and lower Laplace pressure as predicted. The only double-chain surfactant used was SOPC, and since its results do not deviate from the trend for the single-chain surfactant it is not considered to affect the dissolution any differently. The presence of a vapor pressure of the surrounding medium in the microbubble offsets part of the solute pressure and accordingly reduces the gas solute concentration at the interface and hinders the rate of shrinkage but has shown to be much less significant than surface tension.[40] Kloek et al. have recently shown the effects that bulk and interfacial rheological properties have on the dissolution behavior of a single bubble in an infinite medium.[42] However, these are more important for food systems where the viscosity and/or elasticity are much higher than those of the air/surfactant or monomolecular lipid shell/water system presented here. Thus these properties of viscosity and/or elasticity are relatively insignificant to the systems explored in this paper. All of these effects have been shown not to be major factors in the dissolution of a microbubble this small in size; however, collectively they may contribute to the slight deviation found in the experiment from the theory. Nevertheless, the analytical EP solution is shown to be a good approximation of the experiment.

Previously, others have compared the numerical results from exact mass transfer equations to the quasi-stationary approximation of Epstein−Plesset as presented in this paper. Weinberg observed that the approximation dissolution time is only 1% faster than the exact mass transfer equations and that surface tension is the greatest factor, compared with all convection effects, for the entire dissolution of a small air bubble in saturated solution.[41] Yung et al. also compared the numerical result with the Epstein−Plesset approximation for inclusion of surface tension and water vapor in the bubble.[40] They found that the results of the approximations are very close to their more exact numerical results except when the bubble is closer to complete dissolution where the approximation methods predict a lower radius (the approximation starts to deviate after the radius is about 50% of the initial radius). Surface tension and solvent vapor are found to be important when the liquid is slightly undersaturated with the diffusing gases. When undersaturation is large, both effects can be neglected and the approximate methods and the numerical solutions are equally effective in matching the experimental data. This is in agreement with our result of the EP theory slightly underpredicting the experimental data.

Effect of Undersaturation (Experiment II). The aim of experiment II was to study the effect of air undersaturation on air-filled microparticle dissolution and compare to EP theory. To study the effect of undersaturation independently, the interface must have zero tension in the surface. To accomplish this, gel-phase lipids were used to achieve zero tension in the surface and thus zero Laplace overpressure. For a solid lipid shell coated microparticle, the term "tension in the surface" is used to distinguish from the "free" surface tension. This tension in the surface determines the excess pressure in the solid lipid coated microparticle case (experiment II). A solid lipid shell can sustain a state of stress in the surface, particularly as the monolayer transition temperature is much higher than ambient temperature. Direct mechanical tensions can be applied that are not necessarily the same as thermodynamic surface tensions involving free partitioning of interfacial surfactants and phases.

For a gas microparticle that has a monolayer of surfactant, especially a waxy (solid) lipid shell at its interface, it might be expected that the monolayer would present a barrier to gas diffusion out of the particle, and so a second diffusion constant (or resistance) may have to be included in series with gas diffusion in the surrounding solution. A single layer of molecules, particularly if they are largely lipid in makeup, may slow permeation of some gases, but gases with high lipid solubility would have their diffusion enhanced by a lipid monolayer.[67] It has been shown by a variety of techniques that monolayers of the

(67) Blank, M. The permeability of monolayers to several gases. In *Retardation of Evaporation by Monolayers*: *Transport Processes*; LaMer, V. K., Ed.; Academic Press: New York, 1962.

close-packed condensed type, such as fatty acids and alcohols of saturated C16 chain length and longer, lower the evaporation rate. Monolayers such as oleic acid, cholesterol, and various protein films have no detectable effect. In general, the effectiveness of close-packed monolayers is related to the size and shape of the hydrocarbon chain and to the nature of the polar group. We have shown here that the use of a solid lipid shell can eliminate the Laplace driving overpressure and therefore these waxy monolayer-coated interfaces exist with zero tension at the air/water interface. That is, considering the fact that the encapsulated gas microparticle in saturated solution ($f = 1$) is stable, the tension in the surface must be zero. Otherwise, from Epstein−Plesset theory, the encapsulated gas microparticle would have dissolved very rapidly, in seconds, as do free gas microbubbles (see experiment I). Even if the surface tension was only 5 mN/m in a saturated solution, a $R_0 = 15\ \mu$m gas microparticle would theoretically dissolve in about 5 min; however, again we have shown it does not change size for at least 6 h.

The micropipet technique allows near isotropic diffusion of the microparticle gas, since it is free of an impermeable wall. This is consistent with the EP theory, and one can now use this technique to make absolute conclusions. Borden and Longo have shown a relative monotonic increase in shell resistance to gas dissolution with increase of lipid hydrophobic chain length (diC18PC−diC24PC), while finding a near constant level of resistance for chain length diC18PC and lower.[33] As shown in Figure 12, an impermeable wall increases the dissolution time by 44%. If not accounted for, this large increase in dissolution time would be erroneously attributed to a resistance due to the monolayer. After subtracting the resistance due to the impermeable glass wall from the results of Borden and Longo, it can be concluded that no resistance is encountered with lipid chain lengths below diC18PC and an increase of resistance exists with lipid chain lengths from diC18PC to diC24PC (with a slope equal to their results). Using the micropipet technique, we have shown that DSPC (diC18PC) does not have a resistance to gas diffusion out of the microparticle. In processing gas microparticles, we had a constant cooling rate for taking the DSPC shells through their liquid crystalline to solid phase transition at 55 °C and thus consistent microstructure and mechanical properties,[36,39] and as the data presented here suggest, the diC18PC solid shell does not hinder gas dissolution. Compared to our data, Borden and Longo's resistance measurements (once corrected for the boundary effects) would represent the true dissolution time and the resistance provided by PC lipid shells.

The average experimental error of experiment II was calculated to be 3.2% (percent standard deviation). This is compared to an experimental error of over 35% found previously by others using lipid DSPC at the interface of the microparticle.[33] Without fitting, the theory overpredicts experiment II by an average of 8.2% as shown in Figure 11. This is only an average of about a 4.1 s shift in total dissolution time from the theory. The slight deviation of the experiment from the theory could be contributed by convection effects that were not incorporated in the original approximate theory. Even though the convection effects were shown to be insignificant overall, they are a large amount of the relatively small deviation of the theory. Including convection effects would shift the theory to lower dissolution times and more closely align the theory to the experimental data. The convection effects would impose only a 1−4% overall shift but nonetheless would shift the theory closer. While no single explanation can be found for the reason both experiment I and experiment II were slightly different from their respective theories, they have both proved to be very good approximations. The experimental technique is very consistent and reproducible as shown by the low experimental error.

Conclusion

The Epstein and Plesset model is found to be a good approximation for the complete dissolution of a small (less than 15 μm radius) gas microparticle in aqueous solution. The micropipet technique has shown to provide a very appropriate and relatively convenient method with which to test the Epstein−Plesset theory because of the fact that there are no large solid boundaries that create nonisotropic diffusion and concentration fields and that individual microparticles and microbubbles could either be created in situ in saturated solution (microbubble) or be manipulated into undersaturated solution (gas microparticle). Subsequently, the experimental method has been shown to more appropriately test the required Epstein−Plesset model conditions and assumptions for a single gas microbubble or gas microparticle in an infinite isotropic medium than previous attempts that have contained larger error and ill-defined interfacial conditions. The use of surfactants to control surface tension also allowed control of any contamination that has affected previous experimental attempts. The lifetime of a gas microparticle has been found with the micropipet technique with a 3.2% error, an improvement over previous attempts by others. The Epstein−Plesset model slightly underpredicted the dissolution time by 8.6% of the measured dissolution time for experiment I, where the effect of surface tension, and therefore Laplace pressure, was considered (in gas-saturated solution) for a range of surface tensions from 72 down to 25 mN/m. The EP model slightly overpredicted the dissolution time by 8.2% of the measured dissolution time for experiment II, where the effect of undersaturation was considered for a microparticle with zero tension in the surface (zero Laplace pressure) in a range of gas-saturated solutions from 70% to 100%. These data then have allowed us to accurately test the Epstein−Plesset model for the dissolution time of an air microparticle in water.

Acknowledgment. This work was supported by NIH Grant GM 40162. P. Brent Duncan is supported by a fellowship from the Duke University Program in Cellular and Biosurface Engineering. The authors thank Matthew Swingle for his contribution to the initial stage of this research.

Notation

c	gas concentration
C_0	initial gas concentration in the medium
C_s	saturated gas concentration in the medium
t	time
r	radial position
R	microparticle radius
R_0	initial microparticle radius
D	diffusion coefficient
m	mass
J	gas flux
ρ	density of the gas
ρ_b	density of the gas in the bubble
f	medium gas saturation fraction ($f = C_0/C_s$)

k_H	Henry's law constant
P_∞	atmospheric pressure
M_w	molecular weight
B	gas constant
T	temperature
t_d	dissolution time
σ	surface tension
n	number of moles
V	volume
π_c	critical surface pressure
SDS	sodium dodecyl sulfate
DDBSA	dodecyl benzene sulfonic acid
SOPC	stearoyloleoyl-phosphocholine
DSPC	distearoyl-phosphocholine

LA034930I